Effects of Retinal Eccentricity on Human Manual Control

Alexandru Popovici
San Jose State University
NASA Ames Research Center
Moffett Field, CA

Peter M. T. Zaal
San Jose State University
NASA Ames Research Center
Moffett Field, CA

ABSTRACT

This study investigated the effects of viewing a primary flight display at different retinal eccentricities on human manual control behavior and performance. Ten participants performed a pitch tracking task while looking at a simplified primary flight display at different horizontal and vertical retinal eccentricities, and with two different controlled dynamics. Tracking performance declined at higher eccentricity angles and participants behaved more nonlinearly. The visual error rate gain increased with eccentricity for single-integrator-like controlled dynamics, but decreased for double-integrator-like dynamics. Participants' visual time delay was up to 100 ms higher at the highest horizontal eccentricity compared to foveal viewing. Overall, vertical eccentricity had a larger impact than horizontal eccentricity on most of the human manual control parameters and performance. Results might be useful in the design of displays and procedures that increase manual control performance in critical flight conditions such as an aerodynamic stall.

INTRODUCTION

When manually controling an aircraft, pilots often scan a large visual area of the cockpit, while at the same time performing a manual control task. In these situations, it is very likely that pilots will observe the aircraft's attitude on the primary flight display with their peripheral vision. Human manual control in active compensatory tracking tasks is relatively well understood, and it is known that human controllers are able to achieve stable closed-loop performance by adjusting the weights put on the position and rate of the perceived visual cues [1]. Previous experiments using passive observers also showed that the perception of length and velocity is different in peripheral compared to foveal vision [2–5]. With this in mind, the aim of this research was to use a cybernetic approach to investigate the effects of viewing task variables from a display peripherally at different retinal eccentricities in an active manual control task, by modeling human manual control behavior. This approach provides insights into how manual control performance, and the use of visual position and velocity information changes when peripheral vision is used in active manual control tasks.

The paper adds to the literature in two ways. First, it investigates how human manual control parameters are affected by retinal eccentricity using a cybernetic approach. Second, an active control task was used, expanding on results found in previous fundamental vision science experiments with passive observers and visual stimuli presented in a controlled, predefined manner.

PREVIOUS RESEARCH

Past studies have investigated the effects of peripheral vision on position and velocity perception. Tynan et al. found that perceived velocity decreased when eccentricity increased. This effect reduced with higher velocities [6]. Moreover, both the minimum velocity perception threshold and the reaction time to motion onset increased with increased eccentricity. A study that tried to understand the neuro-physical mechanisms behind speed encoding in the periphery found that perceived velocity decreased with eccentricity only at high luminance levels, and sometimes the effect was inverted at very low levels of luminance [2]. Another study also looked at the thresholds for acceleration and deceleration detection of Gabor stimuli at different retinal eccentricities. Traschtz et al. found that at low eccentricities, humans were better at perceiving acceleration, whereas the deceleration thresholds became lower than those for acceleration at higher eccentricities [3]. Stone et al. found that speed perception is also dependent on the contrast of the presented stimuli [4].

Presented at the **IMAGE 2017** Conference
Dayton, Ohio – 27-28 June 2017

Thompson et al. examined the perceived length of a single line in peripheral view. His findings showed that for horizontal lines, the perceived length decreased with both horizontal and vertical eccentricity. For vertical lines, however, the perceived length appeared to decrease only with vertical eccentricity [5].

Some studies investigated the effects of peripheral visual cues on manual control behavior and performance in active control tasks [7, 8]. However, in these studies, peripheral visual stimuli were always present in addition to a central visual display, and the effects of retinal eccentricity were not investigated. In both compensatory target-following and disturbance-rejection manual control tasks, peripheral visual cues were found to increase tracking performance, with only very limited changes in manual control behavior. The effects of peripheral visual cues were more significant in target-following than in disturbance-rejection tasks.

A few observations can be made after analyzing the research presented above. First, in general, length, velocity and acceleration determination is not as good at higher retinal eccentricities. Second, it is clear that speed perception is not only affected by changes in eccentricity, but depends on far more parameters: contrast, luminance, orientation, etc. Furthermore, most of the experiments above took place in very controlled environments, where the visual stimulus speed was maintained constant during runs, with human subjects as passive observers. In an active manual tracking task, the velocity of visual stimuli is highly variable, accelerating and decelerating depending on the human operator's control inputs and the controlled dynamics. In addition, in such an active task, human operators' cognitive load is higher. Because of this, the results found in these passive task experiments might not directly apply to active manual control tasks.

MANUAL CONTROL TASK

A diagram showing the different components of the closed-loop manual control task used in this study is shown in Fig. 1. Here, the human operator has to actively minimize the error e presented on a compensatory display, resembling a primary flight display (PFD), by providing continuous control inputs u with a joystick. These control inputs are transformed into aircraft pitch attitudes θ by the controlled aircraft dynamics $H_c(s)$. The error e is the difference between the actual aircraft pitch attitude θ and a target pitch signal f_i. Human manual control in the compensatory tracking task in Fig. 1 is typically modeled with a linear transfer function $H_p(s)$, and a remnant signal n that captures human nonlinear behavior and noise in the control loop [1]. The spectrum of the human remnant n has the shape of a first order low-pass filter according to Levison [9]. The remainder of this section provides more details on the different components of the control task depicted in Fig. 1.

Controlled Dynamics

The following transfer function was used to simulate the controlled aircraft pitch dynamics:

$$H_c(s) = \frac{K_d}{s(s+\omega_d)} \tag{1}$$

with K_d the gain of the controlled dynamics, and ω_d the break frequency. For values of the break frequency ω_d substantially above the crossover frequency of the human-operator/controlled-dynamics open loop, the dynamics are single-integrator-like and are perceived as easy to control. This is similar to controlling pitch rate. Small values of ω_d, below the crossover frequency, represent more difficult double integrator-like dynamics, corresponding to pitch-acceleration control.

Human Operator Model

McRuer's crossover theorem states a human operator adjusts his/her equalization dynamics to controlled dynamics such that the open-loop human-operator/controlled-dynamics transfer function H_pH_c has the form of a single integrator around the crossover frequency [1]. With the controlled dynamics of Eq. (1), human operators need to provide lead equalization at higher frequencies. Taking this into account, the human operator in Fig. 1 can be characterized using the following transfer function:

$$H_p(s) = \overbrace{K_p[1+T_L s]}^{equalization}\overbrace{e^{-\tau_v s}\frac{\omega_n^2}{\omega_n^2+2\zeta_n\omega_n s+s^2}}^{limitations} \tag{2}$$

Equalization parameters K_p and T_L are the human operator visual gain and lead time constant, respectively. K_p is the relative weight the human operator puts on the error signal (e), and K_pT_L, the relative weight on error rate ($\dot{e}$) in order to achieve stable control in the closed loop. Parameter τ_v represents the time delay associated with visual perception, processing, and neural activation. Parameters ω_n and ζ_n represent the neuromuscular frequency and damping ratio of the combined human arm/hand and control inceptor.

Considering the controlled dynamics of Eq. (1), a human operator needs to generate more lead (higher T_L) for

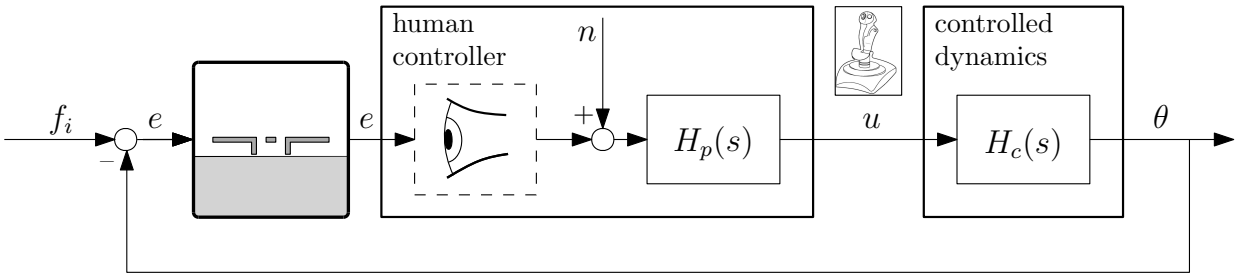

Figure 1 Closed-loop compensatory tracking task.

double-integrator-like dynamics (lower values of ω_d) in order to achieve stable control. The opposite is true for single-integrator-like dynamics, for which less lead generation is required.

Target Signal

To facilitate the identification of the linear transfer function H_p from experimental data, the forcing function f_i in Fig. 1 is typically modeled as a sum of sines, with each sine having a different frequency:

$$f_i(t) = \sum_{k=1}^{N_f} A_f(k) sin[\omega_f(k)t + \phi_f(k)] \qquad (3)$$

with $A_f(k)$, $\omega_f(k)$, and $\phi_f(k)$ the amplitude, frequency and phase of the k^{th} sine in f_i, respectively. N_f represents the number of sine waves, which was 10 in the current study. A summary of all forcing function properties can be found in Table 1.

Table 1 Forcing function properties.

k	n_f	ω_f, rad/s	A_f, deg	ϕ_f, deg
1	6	0.460	6.2472	-84.774
2	13	0.997	4.3688	-4.269
3	27	2.070	1.9712	40.141
4	41	3.144	1.0616	-112.088
5	53	4.065	0.7128	-161.179
6	73	5.599	0.4416	120.470
7	103	7.900	0.2808	-149.989
8	139	10.661	0.2048	129.202
9	174	13.346	0.1712	-38.612
10	229	17.564	0.1456	11.127

The sinusoid frequencies were all integer multiples n_f of the measurement time base frequency, $\omega_m = 2\pi/T_m = 0.0767$ rad/s. $T_m = 81.92$ s was the measurement time used for the experiment. The selected integer multiples were used in a previous experiment and ensured that the ten sinusoid frequencies covered the frequency range of human control at regular intervals on a logarithmic scale. More details on the used forcing function can be found in [10].

EXPERIMENTAL SETUP

Method

Apparatus

The experiment setup is shown in Fig. 2. Participants were seated in front of a display and were instructed to perform the manual control task using a BG Systems joystick located on the right side. A head and chin rest were used to ensure that the distance from the display was identical for all participants. The height of the table on which the display and head rest were mounted could be adjusted, in order to accommodate different participants' heights. The distance from the head rest to the display was set to 14 inches to allow visual stimuli to be presented at predetermined retinal eccentricities. This distance allowed for the largest horizontal eccentricity to be approximately 30 deg, given the size of the monitor.

A simplified PFD of square dimensions was presented at different retinal eccentricities on a 27" Apple monitor having a resolution of 2560 x 1440 pixels. The PFD spanned a field of view of approximately +-5 deg. On the PFD, a line representing the horizon divided the blue color at the top and the dark-brown color at the bottom. An aircraft symbol was fixed in the middle of the PFD. The error e (Fig. 1) was the difference between the horizontal lines of the fixed aircraft symbol and the moving horizon. A small red cross in the middle of the monitor was the fixation point where subjects were instructed to fixate at all times. The position of the PFD changed between the different experimental conditions. The fixation point overlapped with the center black square of the fixed aircraft symbol in the foveal condition. The background

Figure 2 Experimental setup.

Table 2 Experimental Conditions.

cond.	controlled dynamics (DYN)	PFD position (POS)	factor(level)
C1	velocity (SI)	foveal (F)	DYN(1),POS(1)
C2	velocity (SI)	+15 deg horizontally (R)	DYN(1),POS(2)
C3	velocity (SI)	+30 deg horizontally (RR)	DYN(1),POS(3)
C4	velocity (SI)	-15 deg vertically (B)	DYN(1),POS(4)
C5	acceleration (DI)	foveal (F)	DYN(2),POS(1)
C6	acceleration (DI)	+15 deg horizontally (R)	DYN(2),POS(2)
C7	acceleration (DI)	+30 deg horizontally (RR)	DYN(2),POS(3)
C8	acceleration (DI)	-15 deg horizontally (B)	DYN(2),POS(4)

color of the monitor was a shade of dark grey, chosen such that no after-image effects would occur during the experiment. Fig. 3 shows the display with the PFD at all possible eccentricities (Table 2).

Conditions

The experiment had two independent variables: eccentricity angle of the PFD with respect to the fixation point, and the type of controlled dynamics. Four eccentricity angles and two types of controlled dynamics were tested in a full-factorial design. A summary of the total of eight conditions is given in Table 2.

The four positions of the PFD are indicated by F, R, RR, and B in Fig. 3. F represents the foveal condition, R the +15 deg horizontal eccentricity condition (right), RR the

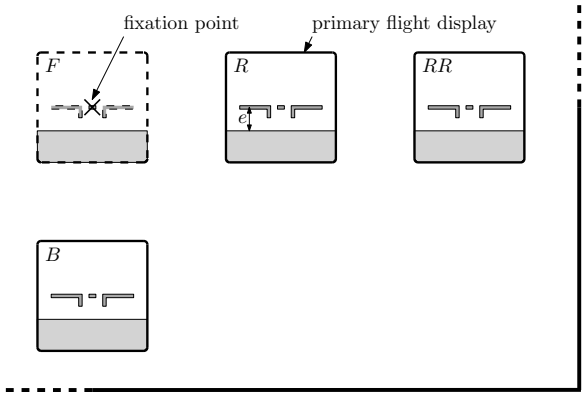

Figure 3 Experimental display.

+30 deg horizontal condition (far right), and B the -15 deg vertical eccentricity condition (bottom). Foveally viewing the control task was the baseline condition. To investigate possible trends in manual control parameters induced by retinal eccentricity, two different horizontal eccentricities were tested. Thirty degrees was the largest achievable eccentricity angle with the experimental setup used. The second horizontal eccentricity was chosen to be half of that. In addition, to investigate the difference between horizontal and vertical eccentricity, a vertical eccentricity was tested with the same angle as the middle horizontal eccentricity (i.e., 15 deg).

The two controlled dynamics are indicated by SI and DI (Table 2). SI represents easier single-integrator-like dynamics ($K_d = 10.5$, $\omega_d = 6.0$ s), whereas DI represents more unstable, double-integrator-like dynamics ($K_d = 4.9$, $\omega_d = 1.0$ s), see Eq. (1). These two controlled dynamics were chosen to provide insights into whether changes in manual control behavior induced by retinal eccentricity depend on the controlled element. The break frequencies (ω_d) of the two controlled dynamics were chosen to achieve the desired variation in control difficulty, after which the gains (K_d) were tuned to create a similar control authority for both. The controlled dynamics were not chosen to be pure single and double integrators in order to estimate the lead time constant more accurately [1, 9]. Furthermore, single-integrator-like dynamics are representative for an aircraft flying under normal conditions, whereas double-integrator-like dynamics occur during unstable flight, in situations such as an aerodynamic stall.

Participants and Procedures

Ten participants between the ages of 22 and 58 participated in the experiment. Four had considerable experience

with manual tracking tasks, one was a commercial pilot, four were general aviation pilots, and one was a graduate student with no prior experience with manual tracking tasks.

Prior to the experiment, participants received a briefing, explaining the task and how to operate the joystick. Participants were instructed to continuously minimize the error on the PFD (i.e., keep the aircraft symbol on the horizon), while fixating on the red cross in the middle of the display and giving smooth, continuous inputs.

Each participant performed a total of 56 runs, 28 for each controlled dynamics. Each run lasted 90 seconds. To minimize the effects of adaptation from one controlled dynamics to another, all runs for a particular controlled dynamics were presented in one segment, followed by all runs for the other dynamics. Half of the participants performed 28 runs of conditions C1-C4 presented according to Latin-square design first, and then 28 runs of conditions C5-C8, also presented according to a Latin-square design. For the other half of the participants, the order of the dynamics was reversed. The first eights runs for each controlled dynamics were used as training and familiarization runs, and were not used for data analysis.

Dependent Variables

The goal of the experiment was to investigate the effects of viewing task variables at different degrees of retinal eccentricity on manual control behavior. Therefore, human control behavior parameters and performance were the variables of interest.

The root mean square (RMS) of the error signal RMS_e was used as a measure for tracking performance. A lower RMS_e indicates better tracking performance. The RMS of the control input RMS_u was used as a measure for control effort. A higher RMS_u indicates a higher control effort.

A time-domain parameter estimation technique based on maximum likelihood estimation was applied in order to obtain the parameters of the human manual control model (Eq. (2)) [11]. Initial parameter estimates were obtained using a genetic algorithm, and refined using a gradient-based Gauss-Newton estimation. Manual control behavior was characterized by the visual error position gain K_p, lead time constant T_L, visual error velocity gain K_pT_L, time delay τ_v, neuromuscular frequency ω_n, and neuromuscular damping ratio ζ_n. The gains K_p and K_pT_L were of particular interest, since they indicate the relative use of error signal position and velocity information, which was expected to vary the most with different eccentricity angles.

The variance accounted for (VAF) is a measure of how much of the measured control input signal u was explained by the linear transfer function H_p. It is an indication of how linearly the human operator behaves, and is typically used as a measure for the goodness of fit of the linear human operator model [11].

Finally, the open-loop crossover frequency ω_c and phase margin φ_m were determined as measures for tracking performance and stability in the frequency domain.

Hypotheses

The main hypotheses of this research revolve around one question: what are the effects of viewing visual information from a PFD at different retinal eccentricities on human manual control behavior? Since past research only investigated the effects of retinal eccentricity in tasks with human subjects as passive observers, the hypotheses formulated here cannot be based solely on findings from these previous studies.

It was hypothesized that increasing the horizontal eccentricity angle would make it harder for the participants to discern the error position. Therefore, it was expected that the visual error position gain K_p would decrease (hypothesis H1). In addition, previous research found velocity perception thresholds increased with larger eccentricity angles. It was expected the visual error velocity gain K_pT_L would increase for increasing eccentricity angles (H2), as participants would need higher gain control inputs to observe a change in the error.

However, previous research also found that perceived velocity decreased with larger eccentricity angles, possibly introducing a limit on the magnitude of K_pT_L at higher eccentricity angles. Therefore, the expected increase in the error velocity gain K_pT_L (as hypothesized in H2) was expected to be reduced or even canceled at higher eccentricity angles (H3). As participants were expected to put a higher gain on error velocity information (higher K_pT_L) for DI-like dynamics compared to SI-like dynamics, this effect was expected to be more dramatic for DI-like dynamics.

Furthermore, conditions C2 and C6, and C4 and C8, had the same angle of eccentricity; however, in the horizontal or vertical axes, respectively. Since the task was a pitch control task, it would be harder to perceive the zero reference line of the fixed aircraft symbol, and thus the magnitude of the error e, when the PFD was below the fixation point. Therefore, it was hypothesized that performance would be lower for conditions C4 and C8 (H4).

Table 3 Main analysis of variance results.

dependent	DYN			POS			DYN×POS		
variable	*df*	*F*	Sig.	*df*	*F*	Sig.	*df*	*F*	Sig.
RMS_e	1.0, 9.0	55.594	**	1.6, 14.6^{gg}	46.707	**	3.0, 27.0	3.773	**
RMS_u	1.0, 9.0	2.711	–	3.0, 27.0	1.943	–	3.0, 27.0	2.289	–
VAF	1.0, 9.0	13.156	**	3.0, 27.0	18.796	**	3.0, 27.0	5.328	**
K_p	1.0, 9.0	50.766	**	3.0, 27.0	51.725	**	3.0, 27.0	21.183	**
T_L	1.0, 9.0	39.281	**	3.0, 27.0	11.686	**	3.0, 27.0	3.780	**
K_pT_L	1.0, 9.0	9.273	**	3.0, 27.0	1.958	–	1.5, 13.7^{gg}	7.813	**
τ_v	1.0, 9.0	0.829	–	3.0, 27.0	29.709	**	3.0, 27.0	2.689	*
ω_n	1.0, 9.0	21.840	**	3.0, 27.0	5.171	**	3.0, 27.0	0.573	–
ζ_n	1.0, 9.0	0.971	–	1.4, 12.9^{gg}	4.872	**	1.1, 10.0^{gg}	4.324	*
ω_c	1.0, 9.0	24.643	**	3.0, 27.0	50.577	**	3.0, 27.0	8.085	**
φ_m	1.0, 9.0	69.875	**	3.0, 27.0	13.369	**	3.0, 27.0	3.335	**

** = significant ($p < 0.05$)
* = marginally significant ($0.05 \leq p < 0.1$)
– = not significant ($p \geq 0.1$)
gg = Greenhouse-Geisser sphericity correction

RESULTS

In this section, significant effects on the dependent variables are discussed. The black solid lines depict data from the conditions with single-integrator-like dynamics (SI), and the grey dotted lines represent the conditions with double-integrator-like dynamics (DI). The error bars indicate the 95% confidence intervals of the mean for all participants, corrected for between-subject variability.

Table 3 provides the results of the two-way repeated measures analysis of variance (ANOVA) performed on the dependent variables of the experiment. As part of the analysis, checks for outliers, normal distribution, and homogeneity of variances were performed. Normality of the data was assessed by Shapiro-Wilk's test of normality. Homogeneity of variances was assessed by Levene's test of equality of variances. As dependent variables contained no outliers and only some were non-normally distributed in only a few conditions, no corrections were applied to the data. Whenever the assumption of homogeneity of variances was violated, a Greenhouse-Geisser correction was used for the degrees of freedom of the F-distribution. For each dependent variable, statistically significant interactions between dynamics and display position are discussed first, if they existed. Statistically significant main effects are discussed only if no statistically significant interactions were found. ANOVA results for simple main effects and post-hoc tests are given throughout the text.

Tracking Performance and Control Activity

Fig. 4a shows participants' tracking performance in terms of the RMS of the error signal. A lower RMS_e means a higher performance. There was a significant two-way interaction between dynamics and position (Table 3). Performance was statistically significantly better for easier SI-like dynamics than DI-like dynamics for all four display positions ($F(1,9) = 36.123, p < 0.001$, $F(1,9) = 32.924, p < 0.001$, $F(1,9) = 33.984, p < 0.001$, $F(1,9) = 28.937, p < 0.001$). In addition, statistically significant differences in performance were found between display positions for both SI-like dynamics ($F(3,27) = 47.665, p < 0.001$), and DI-like dynamics ($F(3,27) = 21.848, p < 0.001$). Post-hoc analysis with Bonferroni adjustment revealed that for the SI-like dynamics performance significantly degraded from foveal to +15 deg horizontal eccentricity ($p < 0.001$) and from +15 deg to +30 deg horizontal eccentricity ($p = 0.005$). Performance was equal between the +30 deg horizontal and -15 deg vertical eccentricity conditions ($p = 1.000$). For the DI-like dynamics, performance decreased from F to R ($p = 0.005$), but was equal between R and RR ($p = 0.279$) and RR and B ($p = 1.000$).

The RMS of the control input is depicted in Fig. 4b. A higher RMS_u means a higher control activity. No statistically significant interaction or statistically significant main effects were found for any of the factors. However, Fig. 4b might suggest that control activity was slightly higher for the DI-like dynamics.

Variance Accounted For

The VAF is depicted in Fig. 5. A significant interaction between DYN and POS was found. The VAF was equal between the two controlled dynamics for the foveal and the +15 deg horizontal eccentricity positions ($F(1,9) = 3.533, p = 0.093$ and $F(1,9) = 0.281, p = 0.609$, respectively). For the +30 deg horizontal eccen-

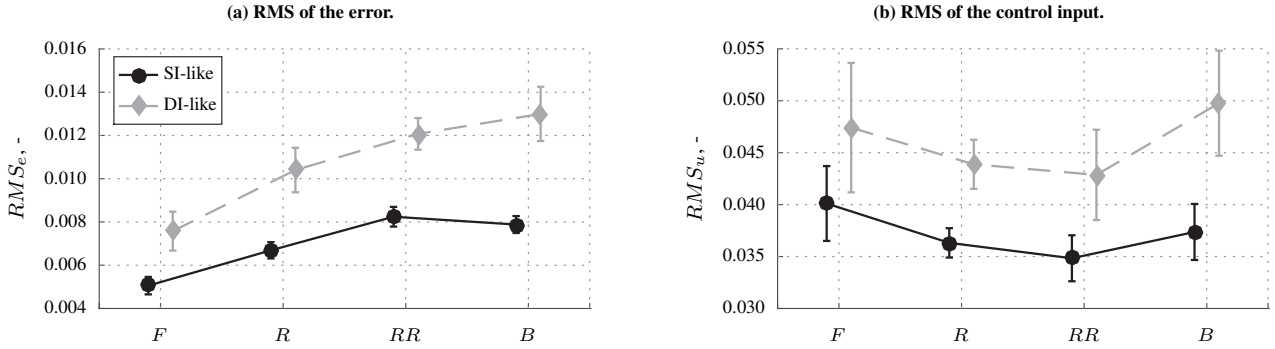

Figure 4 Tracking performance and control activity.

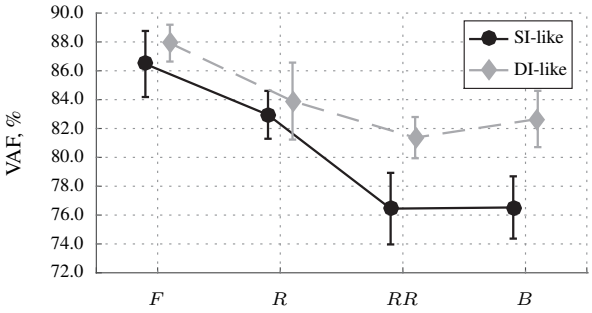

Figure 5 Variance accounted for.

tricity position and the -15 deg vertical eccentricity position, the VAF was statistically significantly higher for the DI-like dynamics ($F(1,9) = 10.959, p = 0.009$ and $F(1,9) = 34.382, p < 0.001$, respectively), indicating that participants behaved more linearly than for the SI-like dynamics. For both the SI-like and the DI-like controlled dynamics, significant differences were found between display positions ($F(3,27) = 20.094, p < 0.001$ and $F(3,27) = 8.439, p < 0.001$, respectively). For the SI-like dynamics, the VAF was equal between the foveal and +15 deg horizontal eccentricity ($p = 0.365$), but then decreased between +15 and +30 deg horizontal eccentricity ($p = 0.007$). The VAF in the -15 deg vertical eccentricity condition was equal to the VAF in the +30 deg horizontal eccentricity condition ($p = 1.000$). The VAF shows a similar trend for the DI-like dynamics. The VAF was equal between F and R ($p = 0.113$), was significantly lower in RR compared to F ($p < 0.001$), and significantly lower in B compared to F ($p = 0.010$). The VAF was equal between R and RR ($p = 1.000$), and RR and B ($p = 1.000$).

Manual Control Behavior

Fig. 6a depicts the human operator gain on visual error position. A significant two-way interaction was found between DYN and POS (Table 3). The visual gain was statistically significantly lower for the DI-like controlled dynamics for all display positions ($F(1,9) = 88.294, p < 0.001$, $F(1,9) = 35.207, p < 0.001$, $F(1,9) = 22.481, p = 0.001$, $F(1,9) = 14.700, p = 0.004$). Statistically significant differences were introduced between display positions for the SI-like dynamics ($F(3,27) = 49.979, p < 0.001$), and the DI-like dynamics ($F(3,27) = 18.034, p < 0.001$). Post-hoc analysis with Bonferroni adjustment revealed that for the SI-like dynamics the gain for position R is significantly smaller than for position F ($p < 0.001$), the gain in RR is smaller than in R ($p = 0.011$), and the gains in RR and B are equal ($p = 1.000$). For the DI-like dynamics, the gain was found to marginally decrease from F to R ($p = 0.076$) and from R to RR ($p = 0.057$), and then significantly increased from RR to B ($p = 0.009$). The visual gain was equal between R and B ($p = 1.000$).

The visual lead time constant is depicted in Fig. 6b. A statistically significant two-way interaction was found between controlled dynamics and display position. A very similar, but opposite trend was observed in T_L compared to K_p. The visual lead time constant was higher for the DI-like dynamics for positions F, R, and RR ($F(1,9) = 169.023, p < 0.001$, $F(1,9) = 35.469, p < 0.001$, $F(1,9) = 21.032, p = 0.001$), indicating an increased reliance on visual rate information. For the -15 deg vertical eccentricity position (B), the visual lead time constant was equal between the two controlled dynamics ($F(1,9) = 1.113, p = 0.319$). For the SI-like dynamics, significant differences were found between different display positions ($F(1.4, 12.9) = 7.553, p = 0.011$). An increasing trend can be observed going from F to

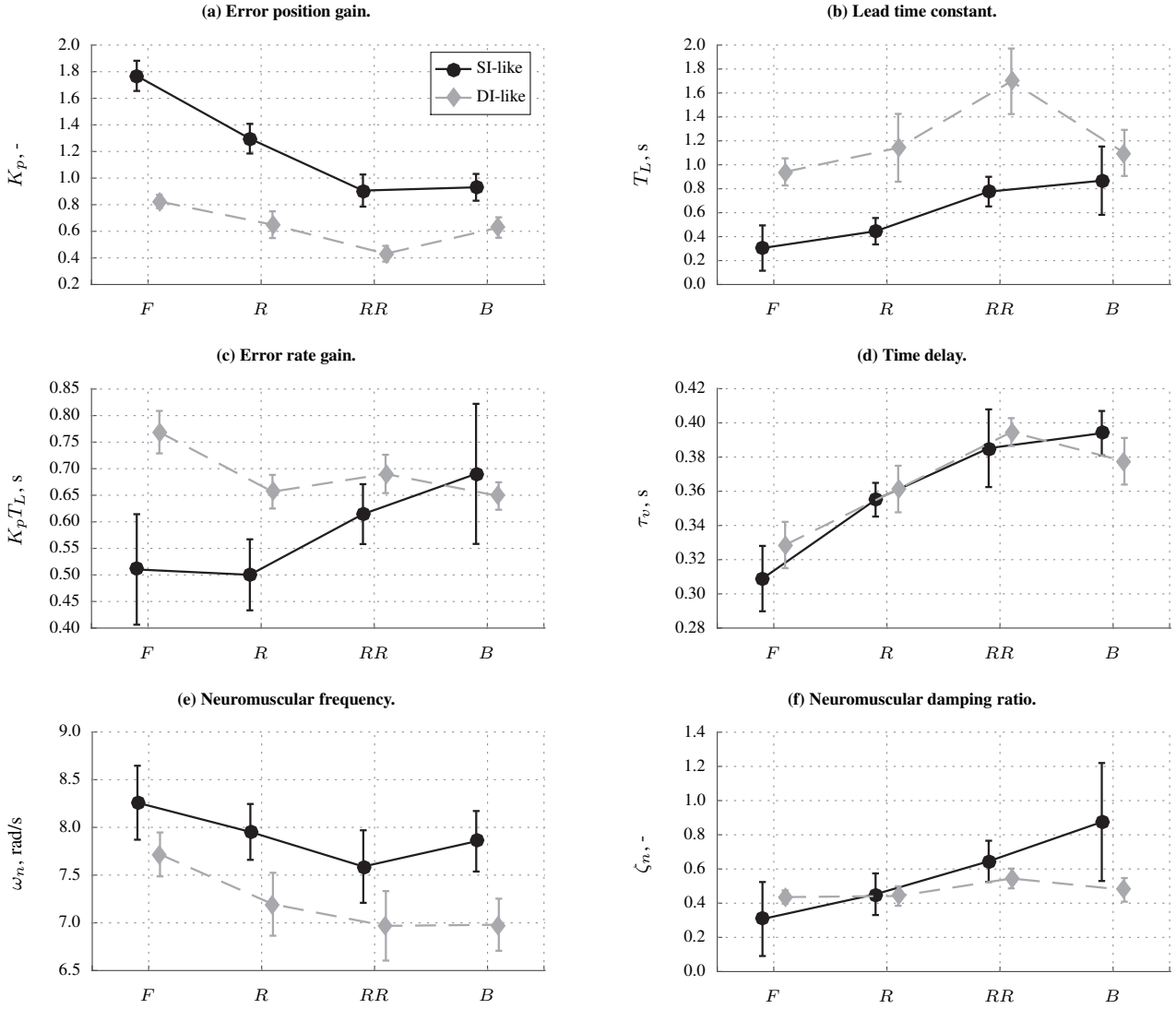

Figure 6 Human controller parameters.

B; however, T_L is found to be statistically significantly higher in RR compared to F and R only ($p = 0.008$ and $p = 0.017$). Significant differences between display positions were also found for the DI-like dynamics ($F(3, 27) = 8.147, p = 0.001$). In this case, T_L was found to be statistically significantly higher in RR compared to F and B only ($p = 0.004$ and $p = 0.033$).

The overall human operator gain on visual error rate (K_pT_L) is depicted in Fig. 6c. Note that this gain is just the multiplication of K_p and T_L. A significant two-way interaction was found for this gain as well. For the foveal and +15 deg horizontal eccentricity positions, the error rate gain was significantly higher for the DI-like dynamics ($F(1, 9) = 30.722, p < 0.001$ and $F(1, 9) = 14.095, p = 0.005$). For the +30 deg horizontal and -15 deg vertical eccentricity positions, K_pT_L was equal between both controlled dynamics ($F(1, 9) = 3.320, p = 0.102$ and $F(1, 9) = 0.290, p = 0.603$). Statistically significant differences were found between the different display positions for both SI- and DI-like dynamics ($F(3, 27) = 3.505, p = 0.029$ and $F(3, 27) = 10.108, p < 0.001$). Post-hoc analysis with Bonferroni adjustment indicated there were no statistically significant differences between any display position pairs for the SI-like controlled dynamics. For the DI-like dynamics, post-hoc analysis revealed that K_pT_L was significantly lower in R and B com-

pared to F ($p = 0.008$ and $p = 0.004$). K_pT_L was equal between F and RR ($p = 0.194$), and R and B ($p = 1.000$).

There was no significant two-way interaction introduced in the visual time delay (Fig. 6d). However, a statistically significant main effect introduced by the display position was found (Table 3). The visual time delay was equal for both dynamics and increased from the foveal to the +15 deg horizontal eccentricity display positions ($p = 0.011$), increased from the +15 deg to the +30 deg horizontal eccentricity positions ($p = 0.008$), and finally remained constant between the +30 deg horizontal and -15 deg vertical eccentricity positions ($p = 1.000$). The difference between the lowest time delay in F and the highest time delay in RR and B was approximately 100 ms.

No statistically significant two-way interaction between DYN and POS was introduced in the human operator's neuromuscular frequency (Fig. 6e). However, the main effects of both DYN and POS were statistically significant. The neuromuscular frequency was significantly higher for the SI-like dynamics compared to the DI-like dynamics (Table 3). Post-hoc analysis with Bonferroni adjustment revealed that the neuromuscular frequency in RR was statistically significantly lower than in F ($p = 0.025$), but was similar between R and F ($p = 0.200$), and B and F ($p = 0.078$), and more similar between R and RR ($p = 1.000$), and R and B ($p = 1.000$).

Fig. 6f depicts the neuromuscular damping ratio. There was no significant two-way interaction introduced in this variable. The main effect of display position was statistically significant. Post-hoc analysis with Bonferroni adjustment revealed that the damping ratio was statistically significantly higher in RR compared to F ($p = 0.035$), but was similar between R and F ($p = 0.354$), and B and F ($p = 0.260$). The neuromuscular damping ratio was also similar between RR and R ($p = 0.279$), and RR and B ($p = 1.000$).

Open-Loop Characteristics

Fig. 7 shows the open-loop crossover frequencies and phase margins. In general, when tracking performance increases, as indicated by an increase in crossover frequency, stability margins decrease; that is, performance is increased by sacrificing stability in the control loop. This effect was also observed in this experiment. A statistically significant two-way interaction between the controlled dynamics and the display position was found in the crossover frequency (Fig. 7a) and phase margin (Fig. 7b). The crossover frequency was statistically significantly lower for the SI-like dynamics for all display positions ($F(1,9) = 9.049, p = 0.015$, $F(1,9) = 14.331, p = 0.004$, $F(1,9) = 23.203, p = 0.001$, $F(1,9) = 41.458, p < 0.001$). The phase margin was statistically significantly higher for the SI-like dynamics for all display positions ($F(1,9) = 153.406, p < 0.001$, $F(1,9) = 49.453, p < 0.001$, $F(1,9) = 14.800, p = 0.004$, $F(1,9) = 31.037, p < 0.001$).

For the both the SI-like and DI-like dynamics, the crossover frequency was statistically significantly different between display positions ($F(3,27) = 52.209, p < 0.001$ and $F(3,27) = 18.417, p < 0.001$). For the SI-like dynamics, the crossover frequency significantly decreased from F to R ($p < 0.001$), and from R to RR ($p = 0.012$), and was equal between RR and B ($p = 1.000$). For the DI-like dynamics, the crossover frequency significantly decreased from F to R ($p = 0.002$), but remained approximately constant between R and RR ($p = 0.225$), and RR and B ($p = 0.247$). The phase margin for the SI-like dynamics was equal between F and R ($p = 0.872$) increased from F to RR ($p = 0.020$), and was equal again between RR and B ($p = 1.000$). For the DI-like dynamics, the phase margin was similar between F and R ($p = 1.000$), and F and B ($p = 0.575$); however was significantly higher in RR compared to F ($p < 0.001$).

DISCUSSION

Human manual control behavior in an active control task was successfully analyzed using a cybernetic approach in experimental conditions with visual stimuli presented at different retinal eccentricities and with two different controlled dynamics. Manual control behavior adapted significantly as visual stimuli were presented at different eccentricity angles, as observed by significant variations in the parameters of the human operator model. Variations in the human control parameters were similar for both controlled dynamics, except for the parameters relating to visual rate information (T_L and K_pT_L).

The human operator visual gain K_p decreased with increasing horizontal eccentricity for both controlled dynamics, as was hypothesized in H1. This reduction in visual gain was most likely caused by the the fact that the visual error was more difficult to discern as the horizontal eccentricity increased. The visual lead time constant T_L increased with increasing horizontal eccentricity, indicating that human controllers relied more on visual rate information as it became harder to observe the error. Combined, these results reflect the fact that velocity is generally easier to perceive in peripheral vision compared to position.

An interesting interaction was observed for the error velocity gain K_pT_L in Fig. 6c. For the SI-like dynam-

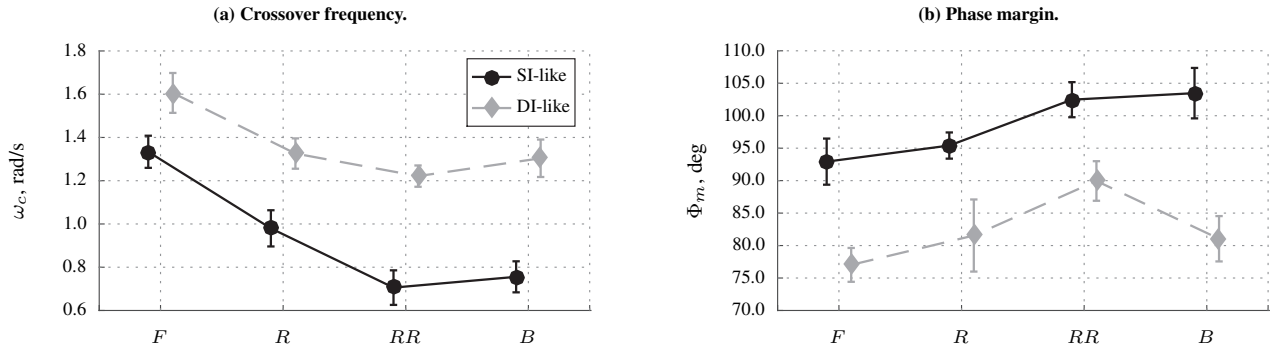

Figure 7 Open-loop performance and stability.

ics, K_pT_L slightly increased with increasing horizontal eccentricity, as hypothesized in H2. However, for the more difficult DI-like dynamics, K_pT_L decreased when using peripheral vision. Furthermore, K_pT_L was equivalent between both controlled dynamics for the +30 deg horizontal and -15 deg vertical eccentricities. Minimum velocity perception thresholds are higher with increased retinal eccentricity [6]. As a result, and with the increased reliance on visual rate information, participants had to increase their gain on visual rate information in order to see changes in visual stimuli. This is reflected in the increase in K_pT_L for the SI-like dynamics. However, at the same time, previous research also found that perceived velocity decreased for increasing eccentricities [2]. It might be that this introduced a limit on the error velocity gain in peripheral vision, resulting in the reduction of K_pT_L for the DI-like dynamics (as hypothesized in H3); that is, as K_pT_L was already higher for the DI-like dynamics compared to SI-like dynamics for foveal vision and above the limit for peripheral vision, it could only go down to the limit value for increasing eccentricities.

The visual time delay and neuromuscular frequency proved to be the human operator limitations most affected by retinal eccentricity. The visual time delay increased with increasing horizontal eccentricity, as also found in previous research [6]. The neuromuscular frequency decreased with increasing horizontal eccentricity, indicating a reduction of the maximum frequency of visual changes acted upon by participants.

The VAF was significantly lower for higher horizontal eccentricities and more so for the SI-like dynamics, indicating participants behaved more nonlinearly. There are a few possible explanations for this. First, higher frequencies are less visible at larger angles of eccentricity, therefore the human controller will react less strongly to these frequencies (as observed in the neuromuscular frequency), making his/her behavior more nonlinear. Second, since minimum velocity thresholds are higher at higher eccentricities, participants might have applied higher gain inputs in order to perceive changes in error velocity. These additional inputs are not correlated with the target signal f_i and will reflect as nonlinear behavior, decreasing the value of the VAF.

The above-discussed changes in human manual control parameters and linearity of control behavior when using peripheral vision resulted in reduced tracking performance at higher eccentricities, as observed by higher values for RMS_e and lower values for ω_c. The reduction in performance was accompanied by an increase in stability margins.

Conditions R and B had the same eccentricity angles, but in the horizontal and vertical axes, respectively. Despite the fact that the eccentricity angles were equal between these two conditions, the two conditions were quite different in nature because of the type of control task and the display used. First, for horizontal eccentricities, the zero-angle reference of the error was easier to discern than for vertical eccentricities, as it was in line with the fixation point. Second, for vertical eccentricities, the error moved towards and away from the fixation point, and, therefore, the instantaneous eccentricity angle varied, whereas it was constant for horizontal eccentricities. Hypothesis H4 stated that the performance was expected to be worse in B compared to R, despite the equivalence in eccentricity angles. This was confirmed in Fig. 4a, where the worst performance was seen in RR and B for both controlled dynamics. In fact, for most dependent variables B was more similar to RR, which indicates that in this pitch tracking task, the -15 deg vertical eccentricity condition had a bigger impact on manual control behavior and performance than the +15 deg horizontal eccentricity condition. For

different control tasks and displays, these effects will most likely be different.

From a practical standpoint, a few lessons can be learned from this study. The time delay, as observed in Fig. 6d, increased up to 100 ms with increasing eccentricities. This can be crucial during critical flight scenarios where reaction time is important, especially as reaction times in such scenarios can already be higher because pilots' increased cognitive load. Second, the results showed that in pitch tracking tasks, viewing the PFD with a vertical eccentricity angle results in lower performance compared to viewing the task with the same horizontal eccentricity angle. Furthermore, participants behaved more nonlinearly at higher eccentricity angles, indicating that pilots could possibly exacerbate unstable flight conditions, such as an aerodynamics stall, when viewing the PFD peripherally. These results could be used to improve the design of human-centered displays and cockpit layouts.

CONCLUSIONS

This paper investigated the effects of retinal eccentricity on human manual control behavior. Ten participants performed a pitch tracking task while looking at a simplified primary flight display at different angles of horizontal and vertical eccentricity, and with two different controlled dynamics. Error position gain generally decreased with increased eccentricity. Error velocity gain increased with eccentricity for the single integrator-like dynamics and decreased for the double integrator-like dynamics, effects which might be linked to higher minimum velocity perception thresholds and decreased perceived velocity in peripheral vision. Vertical eccentricity resulted in a larger impact on control behavior and lower performance than equivalent horizontal eccentricity, as control behavior and performance in the -15 deg vertical eccentricity condition was most similar to the +30 deg horizontal eccentricity condition. The human operator time delay was up to 100 ms higher at higher eccentricities compared to foveal vision. Furthermore, participants behaved more nonlinearly at higher eccentricity angles. The experiment provided important insights into human manual control and performance using peripheral vision, which could be considered in the design of human-centered displays and cockpit layouts.

REFERENCES

[1] D. T. McRuer and H. R. Jex, "A Review of Quasi-Linear Pilot Models," *IEEE Transactions on Human Factors in Electronics*, vol. HFE-8, no. 3, pp. 231–249, 1967.

[2] O. Hassan, P. Thompson, and S. T. Hammett, "Perceived Speed in Peripheral Vision Can Go Up or Down," *Journal of Vision*, vol. 16, no. 6, p. 20, apr 2016.

[3] A. Traschütz, W. Zinke, and D. Wegener, "Speed Change Detection in Foveal and Peripheral Vision," *Vision Research*, vol. 72, pp. 1–13, nov 2012.

[4] L. S. Stone and P. Thompson, "Human speed perception is contrast dependent," *Vision Research*, vol. 32, no. 8, pp. 1535–1549, aug 1992.

[5] J. G. Thompson and K. A. Fowler, "The effects of retinal eccentricity and orientation on perceived length," *The Journal of General Psychology*, vol. 103, no. 2, pp. 227–232, oct 1980.

[6] P. D. Tynan and R. Sekuler, "Motion Processing in Peripheral Vision: Reaction Time and Perceived Velocity," *Vision Research*, vol. 22, no. 1, pp. 61–68, jan 1982.

[7] R. J. A. W. Hosman and J. C. van der Vaart, "Effects of Vestibular and Visual Motion Perception on Task Performance," *Acta Psychologica*, vol. 48, pp. 271–287, 1981.

[8] D. M. Pool, M. Mulder, M. M. van Paassen, and J. C. van der Vaart, "Effects of Peripheral Visual and Physical Motion Cues in Roll-Axis Tracking Tasks," *Journal of Guidance, Control, and Dynamics*, vol. 31, no. 6, pp. 1608–1622, Nov.–Dec. 2008.

[9] W. Levison, S. Baron, and D. Kleinman, "A Model for Human Controller Remnant," *IEEE Transactions on Man Machine Systems*, vol. 10, no. 4, pp. 101–108, Dec. 1969.

[10] A. Popovici, P. Zaal, D. M. Pool, and M. Mulder, "Effects of eye parameters on human controller remnant and control behavior," in *AIAA Modeling and Simulation Technologies Conference*. American Institute of Aeronautics and Astronautics, Jan. 2017.

[11] P. M. T. Zaal, D. M. Pool, Q. P. Chu, M. M. van Paassen, M. Mulder, and J. A. Mulder, "Modeling Human Multimodal Perception and Control Using Genetic Maximum Likelihood Estimation," *Journal of Guidance, Control, and Dynamics*, vol. 32, no. 4, pp. 1089–1099, Jul.–Aug. 2009.